Chemical Engineering Journal 345 (2018) 196–208

Contents lists available at ScienceDirect

Chemical Engineering Journal

journal homepage: www.elsevier.com/locate/cej

Transient effectiveness factor. Simultaneous determination of kinetic, diffusion and adsorption equilibrium parameters in porous catalyst particles under diffusion control conditions

Claudia María Bidabehere[a,*], Juan Rafael García[b], Ulises Sedran[b]

[a] Instituto de Investigaciones en Ciencia y Tecnología de Materiales, INTEMA (UNMDP–CONICET), Juan B. Justo 4302, 7600 Mar del Plata, Argentina
[b] Instituto de Investigaciones en Catálisis y Petroquímica, INCAPE (UNL–CONICET), Colectora Ruta Nac. N° 168 km 0, Paraje El Pozo, 3000 Santa Fe, Argentina

HIGHLIGHTS

- The concept of transient effectiveness factor TEF is applied to kinetic studies.
- TEF allows analyzing the evolutions of reactant concentrations in batch reactors.
- Kinetic, diffusion and adsorption parameters are determined simultaneously.
- A few catalytic experiments in a well stirred batch reactor are needed.
- The approach is more general than those resulting from steady state assumptions.

GRAPHICAL ABSTRACT

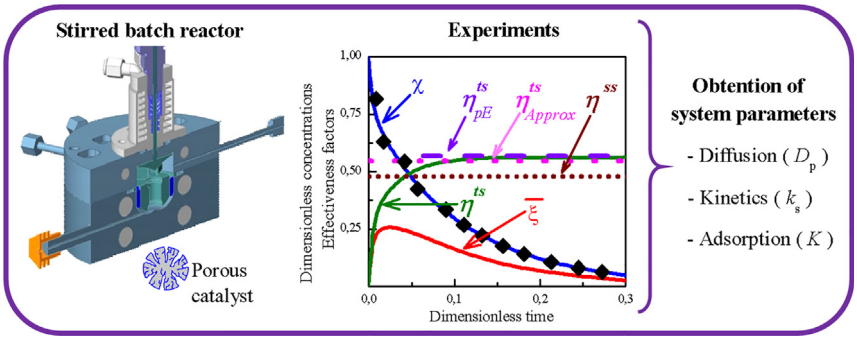

ARTICLE INFO

Keywords:
Porous catalysts
Diffusion-adsorption-reaction
Reactor dynamics
Transient effectiveness factor
Weisz-Prater parameter

ABSTRACT

A method to determine kinetics, diffusion and adsorption equilibrium parameters simultaneously in porous catalyst particles, where a first order chemical reaction occurs under diffusion control conditions in batch reactor, was proposed. The method is based on the use of observable magnitudes from a few experiments in a well stirred batch reactor. By means of a model considering the accumulation of reactant in the catalyst particles, the transient effectiveness factor allows analyzing the time response of systems with different adsorption capacities. The analysis basis and consequent methodology are more general and precise that those resulting from the conventional assumption, which consider that the concentration profiles in the particles, fulfill the steady state condition. Once an initial period elapsed after the reactant injection, the transient effectiveness factor reaches a pseudo-equilibrium state, condition under which an analytical expression can be used to describe the evolution of the reactant concentration in the fluid phase as a function of time. The parameters characterizing that expression of the dynamic response of the reactor, i.e., the exponential decaying constant and the concentration extrapolated at time zero, allow using data from a few experiments to determine the corresponding system's diffusion, adsorption and chemical reaction parameters under reaction conditions.

1. Introduction

Solid porous catalysts are usually prepared in the form of small crystals that are later agglomerated into particles with various shapes in order to ease its use in chemical reactors. Consequently, various steps can be distinguished in the overall process of a chemical reaction

* Corresponding author.
E-mail addresses: cmbidabe@fi.mdp.edu.ar (C.M. Bidabehere), jgarcia@fiq.unl.edu.ar (J.R. García), usedran@fiq.unl.edu.ar (U. Sedran).

https://doi.org/10.1016/j.cej.2018.03.141
Received 27 December 2017; Received in revised form 2 March 2018; Accepted 25 March 2018
Available online 27 March 2018
1385-8947/ © 2018 Elsevier B.V. All rights reserved.

Notation

Symbols

C	Reactant concentration (gmol/m^3)
D	Diffusivity (m^2/s)
F	Function of Thiele modulus for the smallest particles given by Eq. (19)
f	Function
I	Correction factor given by Eq. (9) (dimensionless)
K	Henry's constant (dimensionless).
k	Reaction rate constant (1/s)
m	Mass (kg)
m	Relationship between particle sizes (dimensionless)
Q	Concentration in the solid phase, adsorbed compounds (gmol/m^3)
R	Catalyst particle radius (m)
r	Radial distance (m)
r	Reaction rate per unit volume of porous catalyst particles (gmol/m^{3}s)
s	Coefficients of expansion in Eq. (B.7), defined in Eq. (B.8) (dimensionless)
t	Time (s)
V	Volume (m^3)

Greek symbols

α	System's adsorption capacity defined by Eq. (A.10) (dimensionless)
χ	Dimensionless concentration in the fluid phase of the reactor
ε	Porosity (dimensionless)
ϕ	Thiele modulus (dimensionless)
η	Effectiveness factor (dimensionless)
λ	Eigenvalues in Eq. (B.7), defined in Eq. (B.9) (dimensionless)
θ	Weisz-Prater parameter (dimensionless)
ρ	Dimensionless radial distance
τ	Dimensionless time
ξ	Dimensionless concentration in solid phase

Subscripts

1	Refers to experiments performed with the smallest particles
2	Refers to experiments performed with the biggest particles
a	Adsorption
Approx	Approximate
c	Catalyst
e	Equivalent or effective
f	Fluid phase
i	Order of coefficients s_i in Eq. (B.8)
I	Refers to experiments performed with the highest load of catalyst
II	Refers to experiments performed with the lowest load of catalyst
n	Order of the eigenvalues in Eq. (B.9)
0	At time zero
obs	Observed
p	Particle
pE	Pseudo-equilibrium
R	Reactor
s	Solid phase
TIPB	1,3,5-tri-isopropylbenzene, reactant

Superscripts

–	Volume averaged variable
*	Extrapolation to time zero of the concentration (and dimensionless concentration) in the fluid phase defined by Eq. (10))
o	Initial
ss	Steady state
ts	Transient state

occurring in those catalyst particles: transport of reactants from the bulk of the fluid phase to the external surface of the particles, diffusion through the porous system to the inner sections of the particles, adsorption and desorption, and reaction of the adsorbed reactants. The inverse sequence can be drawn for the products.

The efficiency in the operation of a chemical reactor depends on many issues but, in relation to the solid catalyst, the characteristics of the adsorption equilibrium, the chemical reaction kinetics, the resistances to mass transfer in different locations, and the relative magnitudes of the capacities of the solid and fluid phases to retain reactant can be mentioned. In many cases the chemical reaction rate and the diffusion processes are slow as compared to the adsorption-desorption events and an equilibrium between adsorbed species and molecules in the fluid phase can be assumed [1]. Thus, the assessment of the individual transport, adsorption and chemical reaction parameters is a key issue in reactor analysis and design, many laboratory techniques having been developed to determine them, which have advantages and disadvantages [2,3]. For instance, the recently introduced microimaging infrared microscopy technique can be mentioned [4]. By means of this advanced technique, it is possible to know the transient concentration profiles resulting from diffusion and reaction processes in a one-piece catalyst wafer after a step perturbation in the concentration of reactant in the inlet stream of a flow reactor. Then, the intrinsic diffusivities and chemical reaction rate constants are determined.

Well stirred reactors are frequently used in kinetic studies given some inherent benefits, particularly the lack of temperature and concentration gradients external to the catalyst particles [5], which allows focusing on the diffusion mass transfer process in the pores.One of the basic assumptions in the analysis of chemical kinetics data is that, provided catalyst deactivation is negligible, a steady state can be assigned to the concentration profiles in the catalyst particles, that is, the accumulation terms in the mass balances are neglected [6,7]. Together with the fundamental concept of effectiveness factor (η^{ss}, [6]), the Weisz-Prater parameter (θ, [8]) is a tool usually employed in chemical reaction kinetics analysis by means of which the chemical reaction rate constants (k_s) can be determined from experimental observations, provided the equilibrium adsorption constant (K) and the effective particle diffusivity (D_p) are known [1]. However, it has been shown that the assumption of steady state in the particles is only valid in systems where the adsorption capacity $\alpha = \frac{V_p K_e}{V_f}$, that is, the relationship between the amount of reactant which can be retained in the solid and the fluid phase, respectively, is very low [9]. This fact makes the individual determination of k_s (the first order kinetic constant) and K (the Henry's adsorption constant) impossible and, in order to overcome this point, α should be increased in the experiments [9]; for instance, by increasing the load of catalyst in the batch reactor. Recently, a pseudo-homogenous model for batch reactors has been developed based on the concept of transient effectiveness factor (η^{ts}), which allows these tools to be used in systems where the adsorption capacities are not negligible [10,11]. Again considering that K and D_p are known, this novel model contemplates the accumulation of reactant in the catalyst particles, predicts a constant value for the transient effectiveness factor after a

certain time has elapsed and allows determining k_s from experimental observations, even though the steady state conditions are not fulfilled. If the classical approach (which considers steady state in particles) is assumed and the accumulation term in the mass balance is not negligible, errors can be important [11].

It is the objective of this work to show that the pseudo-homogeneous model is the basis for a new methodology to simultaneously determine k_s, K and D_p in systems with different adsorption capacities, using data from a few laboratory experiments with a catalytic, well stirred batch reactor.

2. Theoretical model

The dynamic response of a reacting system with the following assumptions and conditions is analyzed. The reactor is a well stirred batch reactor where a pulse of reactant is injected over spherical, uniform size catalyst particles. Two phases can be distinguished for the reactant, one diffusing through the particle pores, the other adsorbed on the catalytic surface. The adsorption and desorption rates are much faster than those of the diffusion (Fick's law-type) and first order chemical reaction processes; then, a linear (Henry's law-type) adsorption equilibrium is assumed. The operation is isothermal and the resistance to the mass transfer external to the catalyst particles and the catalyst deactivation are neglected. All the necessary equation developments and variable and parameters definitions are extensively described in Notation, Appendix A and Appendix B sections.

The reactant mass balances in the catalyst particles and the reactor can be respectively described by means of the following dimensionless equations (see Appendix A) [9–11],

$$\frac{\partial \xi}{\partial \tau} = \nabla^2 \xi - \phi^2 \xi \tag{1}$$

$$\frac{d\chi}{d\tau} = -3\alpha \left.\frac{\partial \xi}{\partial \rho}\right|_{\rho=1} \tag{2}$$

and the boundary and initial conditions

$$\left.\frac{\partial \xi}{\partial \rho}\right|_{\rho=0} = 0,\ \xi_{(1,\tau)} = \chi_{(\tau)},\ \xi_{(\rho,0)} = 0,\ \chi_{(0)} = 1 \tag{3}$$

where $\chi = C_f/C_f^o$ represents the dimensionless fluid phase concentration of reactant meanwhile $\xi = C/C_f^o$ is the dimensionless local concentration of reactant in the porous of the catalytic particles. $\tau = tD_e/R^2$ is the dimensionless time and $\rho = r/R$ is the dimensionless radial coordinate. The classical Thiele modulus $\phi = R\sqrt{\frac{k_e}{D_e}}$ and the system's adsorption capacity parameter $\alpha = \frac{V_p K_e}{V_f}$ include the respective diffusion, chemical reaction kinetics and adsorption parameters (see Appendix A)

$$D_e = \frac{D_p}{K_e}, \tag{4}$$

$$k_e = \frac{(1-\varepsilon_p)Kk_s}{K_e} \tag{5}$$

and

$$K_e = \varepsilon_p + (1-\varepsilon_p)K. \tag{6}$$

Examples exist of reactions for which these analysis assumptions are applicable under conditions typical of kinetic studies. Among them, the oxidation of CO [12,13], the biodegradation of phenol [14,15] and the conversion of hydrocarbons in cases where it is possible to distinguish between a diffusing phase and a phase immobilized on the pore's inner surface. Eqs. (1)(3) can still be used in crystals of fine structures such as zeolites provided the expression of the diffusion coefficient is redefined [9].Even though the classical effectiveness factor was defined considering that the concentrations at the external surface and inside the catalyst particles are at the steady state (η^{ss}, which only depends on ϕ [6]), indeed it is always an inherently transient system parameter

$$\eta_{(\tau)} = \frac{\int_0^1 4\pi\rho^2 k_e \xi_{(\rho,\tau)} d\rho}{\frac{4}{3}\pi k_e \chi_{(\tau)}} = \frac{\bar{\xi}_{(\tau)}}{\chi_{(\tau)}} = \eta^{ts}, \tag{7}$$

where $\bar{\xi}$ is the volume averaged concentration of reactant in the pores of the catalyst particles (see Eq. (A.11), Appendix A). The assumption of steady state concentration profiles in the catalyst particles which, mathematically, can be achieved by making nil the accumulation term in the mass balances, has been widely used to represent the reactor's dynamics [7]. However, when the concentration of reactant in the fluid phase changes fast and the system's adsorption capacity is not negligible, the concentration profiles in the particles can not be described properly if the steady state is assumed [9–11].

In a well stirred batch reactor η^{ts} depends not only on the Thiele modulus but also on the system's adsorption capacity (α) [10,11]. Moreover, it was shown that η^{ts} reaches a constant value (η^{ts}_{pE}) once a certain dimensionless time after the injection of reactant has elapsed, thus defining a pseudo-equilibrium state condition [9–11]. Interestingly, such a constant value can be approximated, with a small error, from η^{ss} and the correction factor $I_a(\phi,\alpha)$ (see Eq. (B.16) in Appendix B), which derives from considering the accumulation term in the particles, and includes the characteristic system's dimensionless time constants [10,11],

$$\eta^{ts}_{pE} \cong \eta^{ts}_{Approx} = \eta^{ss} I_a = \eta^{ss}(1 + \tau_p/\tau_{obs}). \tag{8}$$

Here $\tau_p = s_2/s_1$ (where $s_i = \sum_{n=1}^{\infty} 6/(\phi^2 + n^2\pi^2)^i$, see Eqs. (B.8) and (B.9) in Appendix B and [10] is the dimensionless time constant for diffusion, adsorption and reaction in the particles, indicating their inertia in reaching the steady state whose approximate value is $\tau_p \cong 1/(15 + \phi^2)$ [16,17], and $\tau_{obs} = -[d(\ln\chi)/d\tau]^{-1}$ is the observable system's dimensionless characteristic time. It can be seen in Eq. (8) that how much η^{ts}_{pE} differs from η^{ss} depends on the relationship between the corresponding particle and overall inertias.

It can be shown that I_a is a function of α and ϕ (see Appendix B) [10]

$$I_{a\,(\phi,\alpha)} = \frac{(1 + \alpha s_1)}{1 + \alpha s_1 - \alpha s_2 \phi^2}. \tag{9}$$

Fig. 1 shows the evolution of the concentration of reactant in the reactor fluid phase (χ) and the volume-averaged concentration in the particles ($\bar{\xi}$) after the injection. The resulting transient effectiveness factor (η^{ts}, Eq. (7)) and its asymptotic value (η^{ts}_{pE}) are compared with the classical effectiveness factor (η^{ss}, [6]) obtained with the same Thiele modulus assuming the reactant concentrations in the particle are at the

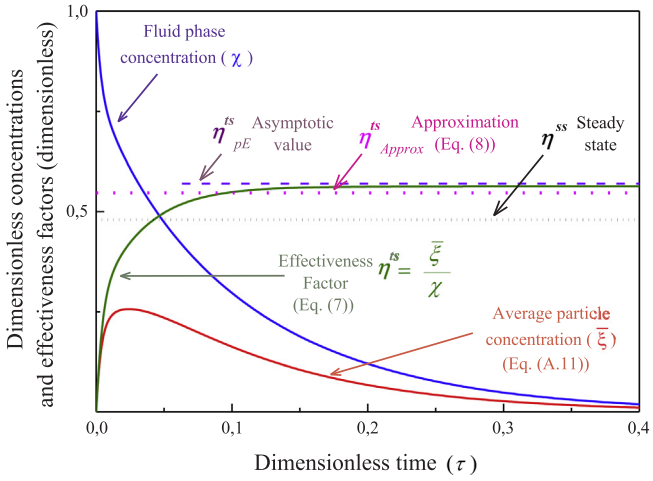

Fig. 1. Evolution of the system concentrations and effectiveness factors as a function of time. ($\phi = 5$; $\alpha = 1$).

steady state. The approximated value (η^{ts}_{Approx}) was calculated after Eqs. (8) and (9).

Accepting that η^{ts} has reached its constant value (η^{ts}_{pE}), then it is possible to find an analytical solution for the evolution of the dimensionless reactant concentration in the reactor's fluid phase, χ [11]

$$\chi = \chi_0^* \exp(-\tau/\tau_{obs}) = \frac{C_0^*}{C_f^o} \exp(-t/t_{obs}), \tag{10}$$

where

$$\chi_0^* = \frac{\exp(\tau_p/\tau_{obs})}{1 + \alpha\eta^{ts}_{pE}} \tag{11}$$

and

$$\tau_{obs} = \frac{1 + \alpha\eta^{ts}_{pE}}{\alpha\eta^{ts}_{pE}\phi^2}. \tag{12}$$

Both the concentration extrapolated to time zero (C_0^*) and the exponential decaying time constant (t_{obs}) can be determined from the experimental observation of the evolution of the reactant concentration in the fluid phase in the reactor (C_f) as a function of reaction time (t) (see Eq. (10)). Fig. 2 shows the evolution of the concentrations as a function of time. For each pair of parameters ϕ and α, the dimensionless concentrations were calculate from the exact solution to the system of Eqs. (1)(3) and Eq. (A.11) (Appendix A). Numerical solutions were obtained by means of a finite difference method with a Crank-Nicholson scheme [18]. Regard to the analytical solutions, the fluid phase dimensionless concentration (χ) was calculated according to Eqs. (10) (12), and the volume averaged concentration in the particle ($\bar{\xi}$) was calculated with Eq. (B.14) (Appendix B) [11]. As it can be seen, in systems where $\alpha \to 0$, the χ value at $\tau \to 0$ is $\chi_0^* \approx 1$ (Fig. 2a and b); however, the larger the α the larger the difference $\chi_0^* < 1$. The approach shows that the closeness of χ_0^* to one is a direct evidence about the validity of the assumption of steady state in the particles [11].

The well-known Weisz-Prater parameter is defined as the relationship between the observed chemical reaction rate per unit volume of catalyst particles (r_{obs}) and a characteristic diffusion rate [1,8]

$$\theta = \frac{R^2}{D_p C_f} r_{obs} \tag{13}$$

which can be conveniently expressed in this case as [11]

$$\theta = \frac{R^2}{D_p}\frac{V_f}{V_p}\frac{1}{t_{obs}}, \quad t_{obs} = -\left[\frac{d\ln(C_f/C_f^o)}{dt}\right]^{-1}. \tag{14}$$

In systems with first order kinetics and linear adsorption equilibrium at the steady state, both η^{ss} and $\theta = \eta^{ss}\phi^2$ only depend on ϕ. However, it has been recently shown that in transient conditions, θ depends not only on ϕ but also on α, according to [11]

$$\theta = \frac{\eta^{ts}_{pE}\phi^2}{1 + \alpha\eta^{ts}_{pE}}. \tag{15}$$

These facts constitute the basis for the individual determination of k_s, D_p and K after a reduced number of simple experiments with a stirred batch catalytic reactor where pulse injections of the reactant are made. Moreover, it is very important to note that the parameters are determined at the actual conditions at which the chemical reaction proceeds.

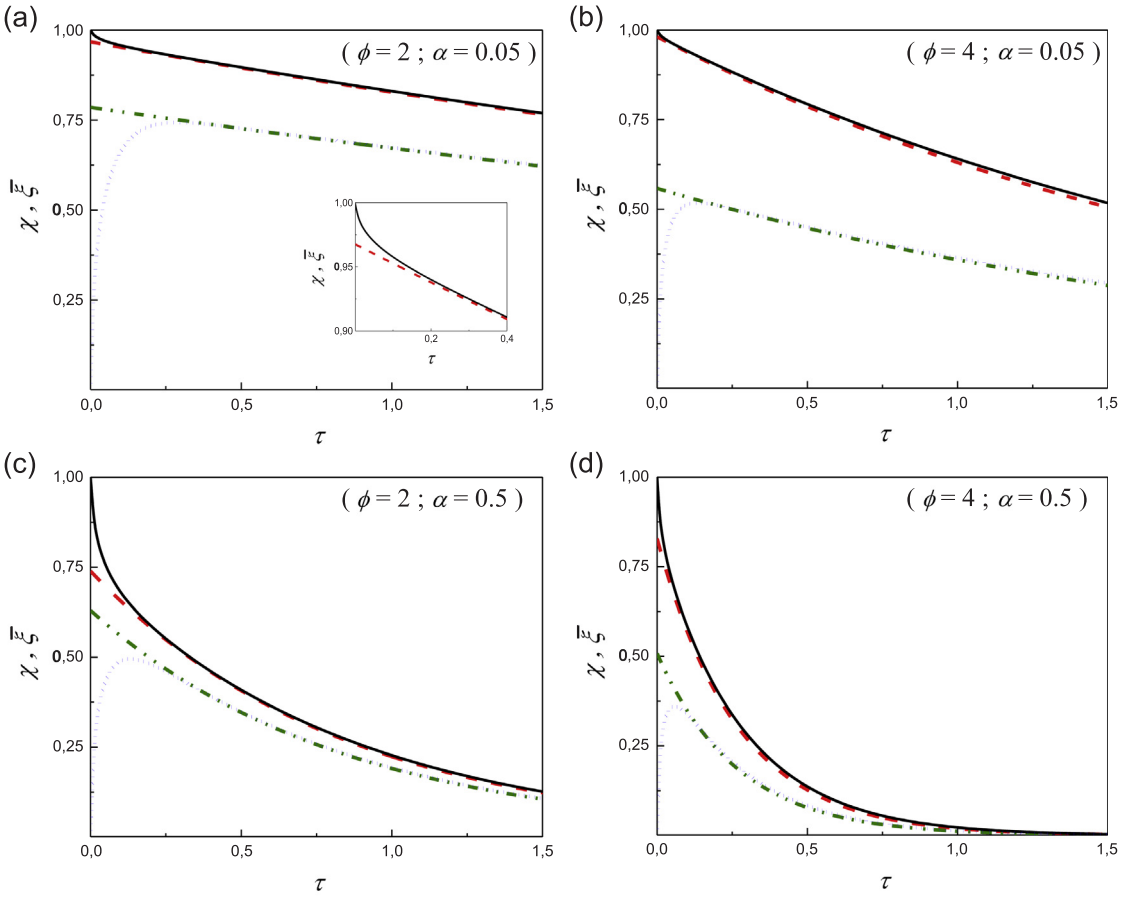

Fig. 2. Dynamic responses in a batch reactor after the injection of a pulse of reactant. Lines: *solid*, χ (exact solution); *dot*, $\bar{\xi}$ (exact solution); *dash*, χ (analytical solution); *dash dot dot*, $\bar{\xi}$ (analytical solution).

3. Results and discussion

3.1. Method's arrangement

If experiments are made in a well stirred batch reactor with different particle sizes, for example $R_2 = m R_1$, of a given catalyst of known porosity (ε_p), the rest of conditions (temperature, catalyst load, initial concentration, etc.) being constant, then $\phi_2 = m\phi_1$ and $\alpha_2 = \alpha_1 = \alpha$. The evolutions of the reactant concentration (C_f) as a function of time (t) are observed in these experiments, the time table of the gathered values allowing to fit them to Eq. (10), that is, the well-known exponential decaying function, so as to determine the two parameters defining it: the concentration extrapolated to time zero (C_0^*) and the exponential decaying time constant (t_{obs}). Moreover, considering Eqs. (A.8) and (A.9) (Appendix A), Eq. (12) can be written as

$$t_{obs} = \frac{1 + \alpha\eta_{pE}^{ts}}{\alpha\,\eta_{pE}^{ts}\,k_e}. \tag{16}$$

The results in the set of Experiments 1 (particle size R_1) and 2 (particle size $R_2 = m R_1$) will yield the concentrations extrapolated to time zero (C_{01}^* and C_{02}^*), and the exponential decaying time constants ($t_{obs\,1}$ and $t_{obs\,2}$), respectively. Then, the relationship between both decaying time constants (see Eq. (16)) is

$$\frac{t_{obs\,2}}{t_{obs\,1}} = \frac{\eta_{pE\,1}^{ts}}{\eta_{pE\,2}^{ts}}\left(\frac{1 + \alpha\eta_{pE\,2}^{ts}}{1 + \alpha\eta_{pE\,1}^{ts}}\right). \tag{17}$$

Following Eq. (8) as applied to both experiments, noticing that $\eta_{pE\,1}^{ts} \cong \eta_{(\phi 1)}^{ss} I_a(\phi_1,\alpha)$ and $\eta_{pE\,2}^{ts} \cong \eta_{(\phi 2)}^{ss} I_a(\phi_2,\alpha)$, Eq. (17) becomes

$$\frac{t_{obs\,2}}{t_{obs\,1}} = \frac{\eta_{(\phi 1)}^{ss}}{\eta_{(\phi 2)}^{ss}}\left[\frac{I_{a\,1}}{I_{a\,2}}\frac{(1 + \alpha\,\eta_{(\phi 2)}^{ss} I_{a\,2})}{(1 + \alpha\,\eta_{(\phi 1)}^{ss} I_{a\,1})}\right]. \tag{18}$$

Moreover, $\phi_2 = m\,\phi_1$ and, given that the conventional effectiveness factor, based on the assumption of steady state, depends only on the Thiele modulus, the relationship $\frac{\eta_{(\phi 1)}^{ss}}{\eta_{(\phi 2)}^{ss}}$ in Eq. (18), which can be expressed analytically, will only include the Thiele modulus for one of the experiments, e.g. ϕ_1, as the unknown parameter. If the particles are spherical, then

$$F(\phi_1) = \frac{\eta_{(\phi 1)}^{ss}}{\eta_{(m\,\phi 1)}^{ss}} = m^2\left(\frac{\phi_1 \coth(\phi_1) - 1}{m\phi_1 \coth(m\phi_1) - 1}\right) \tag{19}$$

and Eq. (18) can be rewritten as

$$\frac{t_{obs\,2}}{t_{obs\,1}} = F(\phi_1)\left[\frac{I_{a\,1}}{I_{a\,2}}\frac{(1 + \alpha\,\eta_{(\phi 2)}^{ss} I_{a\,2})}{(1 + \alpha\,\eta_{(\phi 1)}^{ss} I_{a\,1})}\right]. \tag{20}$$

The following considerations apply in relation to the second parameter defining the evolution of the concentration as a function of time in the fluid phase of the reactor according to the pseudo-homogeneous model, that is, the concentration extrapolated to time zero (C_0^*, see Eq. (10)). Given that the conditions in the experiments imply that the initial concentrations are the same ($C_{f1}^o = C_{f2}^o = C_f^o$), it should be noted that for different Thiele moduli the concentrations extrapolated to time zero are not ($C_{01}^* \neq C_{02}^*$, see Fig. 2). The only particular condition assuring that $C_{01}^* = C_{02}^* = C_f^o$ is that of $\alpha \to 0$, which corresponds to the steady state situation.

It has been shown that in a wide range of ϕ and α values the correction factor I_a will be significantly lower than 2 [10], thus implying that τ_p/τ_{obs} is lower than 1 (see Eq. (8)) and, considering that an exponential function can be approximately expressed as $\exp(x) \cong 1 + x$ (provided $x < 1$), the numerator in Eq. (11) can be written as (see Eq. (8))

$$\exp(\tau_p/\tau_{obs}) \cong 1 + (\tau_p/\tau_{obs}) = I_a. \tag{21}$$

and, consequently,

$$\chi_0^* = \frac{I_a}{1 + \alpha\,\eta^{ss} I_a} = \frac{C_0^*}{C_f^o}. \tag{22}$$

Then,

$$G(\phi_1,\alpha) = \frac{C_{02}^*}{C_{01}^*} = \frac{I_{a\,2}}{I_{a\,1}}\frac{(1 + \alpha\,\eta_{(\phi 1)}^{ss} I_{a\,1})}{(1 + \alpha\,\eta_{(\phi 2)}^{ss} I_{a\,2})}, \tag{23}$$

where $I_{a\,1}(\phi_1,\alpha)$ and $I_{a\,2}(\phi_2,\alpha)$ are given by Eq. (9).

The right hand side in Eq. (23) is the reciprocal of the term between brackets in Eq. (20), and then

$$\frac{t_{obs\,2}}{t_{obs\,1}} = F(\phi_1)\left[\frac{C_{01}^*}{C_{02}^*}\right]. \tag{24}$$

If Eq. (24) is used in Eq. (19),

$$\frac{t_{obs\,2}}{t_{obs\,1}}\frac{C_{02}^*}{C_{01}^*} = m^2\left(\frac{\phi_1 \coth(\phi_1) - 1}{m\phi_1 \coth(m\phi_1) - 1}\right) = F(\phi_1) \tag{25}$$

Now Eq. (25) allows determining the Thiele modulus for the first experiment (ϕ_1), and, consequently, $\phi_2 = m\,\phi_1$. Once ϕ_1 and ϕ_2 are known, Eq. (23) together with Eq. (9) will provide α .

The system's parameters can be now determined. K_e can be calculated with the help of Eq. (A.10) and K with Eq. (6). The constant value of the transient effectiveness factor for the smallest particles ($\eta_{pE\,1}^{ts}$) can be calculated by means of Eq. (7), or approximately by means of Eqs. (8) and (9), and Eq. (15) allows to calculate the corresponding Weisz-Prater parameter (θ_1). Then D_p can be obtained from Eq. (14) using the characteristic time constant t_{obs} determined in the experiments with the particles having R_1 size (i.e., $t_{obs\,1}$). k_e can be calculated according to Eq.

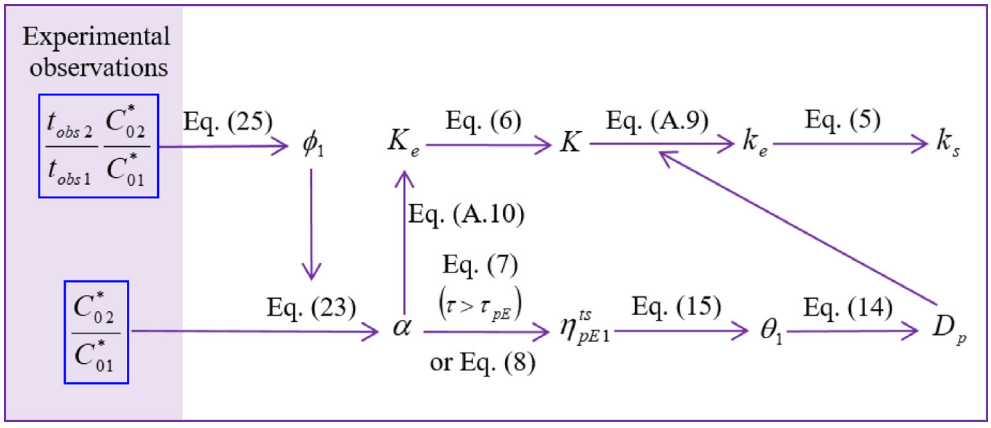

Fig. 3. Scheme of calculations in the method. Parameters R_1, $R_2 = m R_1$, V_f, V_p, ε_p and C_f^o are previously known from the catalytic experiments.

(A.9) and, finally, k_s will be provided by Eq. (5). The flow of calculations in the method is shown in Fig. 3.

An interesting limit case can be discussed. If $\chi^*_{01} = \chi^*_{02} = 1$ (this is the consequence of α being much smaller than one, see Fig. 2a and b), the concentration profiles in the catalyst particles can be considered to be at the steady state and the procedure to determine D_p from magnitudes which can be observed in experiments is the usual one, which is described, e.g., in the textbook by Fogler [1]. However, K and k_s cannot be obtained individually, but their product (Kk_s, [9]). If so, new experiments should be performed at the same temperature with higher catalyst loads and, consequently, higher α values, until $\chi^*_{01} \neq \chi^*_{02} < 1$ is observed, so as to be in position to follow the method described previously.

The method also opens to an attractive option to determine K and k_s provided D_p is previously known. In that case, the batch reactor could be operated with different loads of catalyst particles with the same size, e.g., $V_{pII} = 2\,V_{pI}$ (consequently, $\alpha_{II} = 2\,\alpha_I$), the other conditions being constant. If it is verified that $\chi^*_{0I} \neq \chi^*_{0II} < 1$, then (refer to Eqs. (14) and (15))

$$\frac{\theta_I}{\theta_{II}} = 2\frac{t_{obsII}}{t_{obsI}} = \frac{\eta^{ts}_{pE\,I}}{\eta^{ts}_{pE\,II}}\frac{(1 + 2\alpha_I\eta^{ts}_{pE\,II})}{(1 + \alpha_I\eta^{ts}_{pE\,I})} \tag{26}$$

The only unknown parameter in Eq. (26) is $alpha_I$, since the left hand side is known from the experimental observations (see Eq. (13)), and both $\eta^{ts}_{pE\,I}$ and $\eta^{ts}_{pE\,II}$ can be obtained from θ_I and θ_{II} respectively, according to the methodology recently described in the Ref. [11], where it was shown that the relationship between θ and η^{ts}_{pE} is essentially unique and independent of the value of α. Then α_I can be calculated, and consequently K_e (see Eq. (A.10)) and K (Eq. (6)). Finally, given that now both K and D_p are already known, k_s can be determined following a procedure recently shown by Bidabehere et al. [11] by using the pseudo-homogeneous model here described.

Even though this method was developed, strictly, for systems with irreversible first order kinetics and linear adsorption equilibrium, it is possible to apply it to reactions other than first order, as long as their kinetic expressions could be linearized and described by equations similar to Eqs. (1)(3). It could result in those cases that the kinetic parameters are indeed combinations (for example, $k_sC_TK_L$, when the kinetics is Langmuir-Hinshelwood-Hougen-Watson type $r_s = k_sC_T\left(\frac{K_LC}{1+K_LC}\right)$ [19]).

3.2. Parametric sensitivity and error analysis

The sensitivity and error analysis on the determination of ϕ_1 and α from dimensionless parameters $F(\phi_1) = \frac{t_{obs\,2}}{t_{obs\,1}}\frac{C^*_{02}}{C^*_{01}}$ and $G(\phi_1,\alpha) = \frac{C^*_{02}}{C^*_{01}}$ will show the practical limitations of the method.

Fig. 4 shows the relationship between the Thiele modulus for the smaller particles ϕ_1 and $F(\phi_1)$ (Eq. (19)), for various values of m. Eq. (19) shows that $F(\phi_1)$ is always larger than one, and then two limit situations arise. If $\phi_1 \ll 1$ (that is, no diffusion restrictions), considering that $\eta^{ts}_{pE\,1} \approx \eta^{ts}_{pE\,2} \approx 1$, the curves tend to the asymptotic value $F(\phi_1) = 1$. If $\phi_1 \gg 1$ (that is, neat diffusion control), $\eta^{ts}_{pE\,1} \to \frac{1}{\phi_1}$ and the curves tend to the asymptotic value $F(\phi_1) = m$. It is obvious that in these extreme conditions the curves are near vertical and small errors in the experimental determination of $F(\phi_1)$ (Eq. (25)) may impact severely on the calculated value of ϕ_1. Then, error propagations would be inadmissible if working in those zones.

Fig. 5 shows, for various values of m, the relative errors produced in the calculation of ϕ_1 according to Eq. (19), provided the error in the experimental determination of $F(\phi_1)$ according to Eq. (25) is 5%. It can be seen that for every value of m, covering the range of practical particle size relationships, the values of ϕ_1 leading to small errors are always equal or smaller than 3, suggesting that the effectiveness factor are located in the transition zone. The range of values of $F(\phi_1)$ which guarantee that the relative error in ϕ_1 does not exceed a certain value, for example, 20%, increases together with the particle size relationship m. The lower limit, close to 1.2, is very similar for every m, the upper limits increasing with m (they are close to 1.5, 1.8, 3.7 and 8, when m is 2, 2.38, 5 and 10, respectively).Restrictions on $F(\phi_1)$ provided by Figs. 4 and 5 are necessary but not sufficient, given that, additionally, the correlation between α and ϕ_1 should be as small as possible. Fig. 6 shows the relationship between α and $G(\phi_1,\alpha) = C^*_{02}/C^*_{01}$ for different values of ϕ_1 and m (Eq. (23)). Curves were drawn in the range $0.1 < \alpha < 2$, as prescribed by the method. The upper limit in α insures that the error involved in assuming that the approximation to the pseudo-equilibrium state is correct (Eq. (8)), is smaller than 5% [11]). The consequences of operating under the lower limit ($\alpha < 0.1$) were discussed in Section 3.1. It can be seen in Fig. 6 that α and ϕ_1 are not strongly correlated, thus allowing to use $G(\phi_1,\alpha)$ values to determine α regardless the value of ϕ_1. Moreover, the larger the m (Fig. 6b and c), the smaller the value of ϕ_1 at which α–$G(\phi_1,\alpha)$ does not depends on ϕ_1. This has the additional positive effect of widening the range of admissible $F(\phi_1)$ values (refer to Figs. 4 and 5).

Based on this analysis, the shaded areas in Fig. 7 show the method's operational windows, where the correlation between α and ϕ_1 and the error in the determination of ϕ_1 are minimum. Fig. 7 shows that in all cases ϕ_1 is equal to or less than 3 if low levels of error are desired, thus indicating that the conditions for the experiment with the smaller catalyst should always ensure that the diffusive resistance does not prevail.Fig. 8 shows the values of $F(\phi_1)$ and $G(\phi_1,\alpha)$ as a function of m which lead to reliable determinations of the parameters ϕ_1 and α, thus constituting an operative guide to the proper selection of experimental conditions, which are implicit in Fig. 7. Note that m is known previous to the experiments and that $F(\phi_1)$ and $G(\phi_1,\alpha)$ can be determined directly from experimental results. Different zones in the figure show the different system's adsorption capacities. It should be noted that the larger the restrictions on the $F(\phi_1)$ range, the smaller the restriction on the $G(\phi_1,\alpha)$ range.

3.3. Application example

3.3.1. Experimental

1,3,5-tri-isopropylbenzene (TIPB, Aldrich) was converted at 550 °C over a commercial amorphous mesoporous silica-alumina catalyst (HA-HPV Ketjen, Amsterdam, Netherlands) in order to show the method's application. Catalyst properties are shown in Table 1. The as-received catalyst was sieved and separated into various particle size fractions, two of them being used in the experiments: 200–270 mesh and 80–120

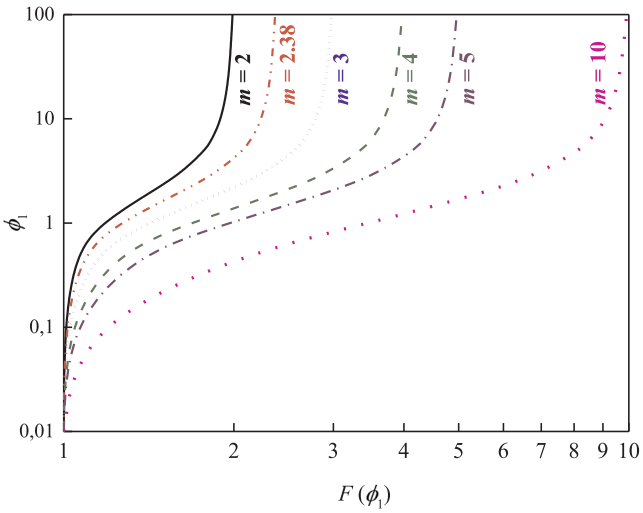

Fig. 4. Thiele modulus for the smallest particles ϕ_1 as a function of $F(\phi_1)$ (Eq. (19)).

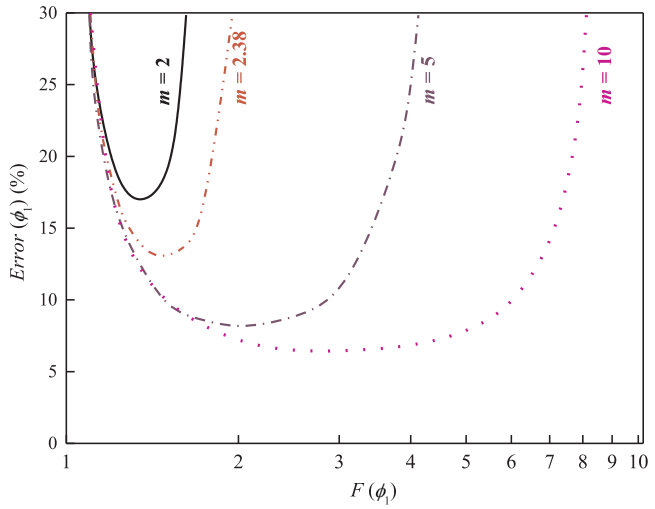

Fig. 5. Error (%) in the determination of ϕ_1 for different values of m when the error in the determination of $F(\phi_1)$ is 5%.

mesh (that is, 53–75 μm and 125–180 μm).

The experiments of conversion of TIPB were performed in a fluidized bed, internal recirculation batch laboratory reactor where the catalyst is confined in a basket between two metal porous plates [20], as it can be seen in Fig. 9. The reactor's configuration allows satisfying essentially all the hypothesis considered in section "System model". The experimental conditions are summarized in Table 2. Once the target temperature and mixing conditions were achieved, a given amount of TIPB was injected to the reactor and the sample was instantaneously vaporized due to the high temperature. Simultaneously to the injection, a timer was started. When the reaction time was reached, a valve connecting the reactor with a large volume evacuation chamber was automatically opened, so that both the products and unreacted TIPB in the reactor were instantly evacuated. Then a sampling loop was filled and the sample was finally injected into a gas chromatograph by means of a six-way valve. The reaction products were analyzed on-line with the help of standard capillary gas chromatography using a non-polar column and flame ionization detection (FID). A 30 m long, 250 μm diameter and 0.25 μm film thickness, non-polar, dimethylpolysiloxane column was used. Coke deposited on the catalyst surface was determined by means of temperature-programmed oxidation and further methanation of the carbon oxides. Methane was quantified with the help of a FID detector. Mass balances (recoveries) closed to ±5% in all the cases.

3.3.2. Determination of system parameters K, D_p and k_s

Catalyst activity was considered constant, given that coke yields were very small in all the experiments. Fig. 10 shows the evolutions of the dimensionless concentration (C_f/C_f^o) observed in the cracking of TIPB at 550 °C over the two different particle sizes, as a function of reaction time (t). Fitting data which satisfy that the η_{pE}^{ts} value has been reached (Eq. (10) was derived under that condition), which ensures the exponential matching with the final portion of the curves concentration versus time curves (see Fig. 2) to Eq. (10), shows that

- Particle size R_1:

$$t_{obs\,1} = 53.480\ s \tag{27}$$

$$\chi_{01}^{*} = C_{01}^{*}/C_f^o = 0.773 \tag{28}$$

$$R^2 = 0.9998 \tag{29}$$

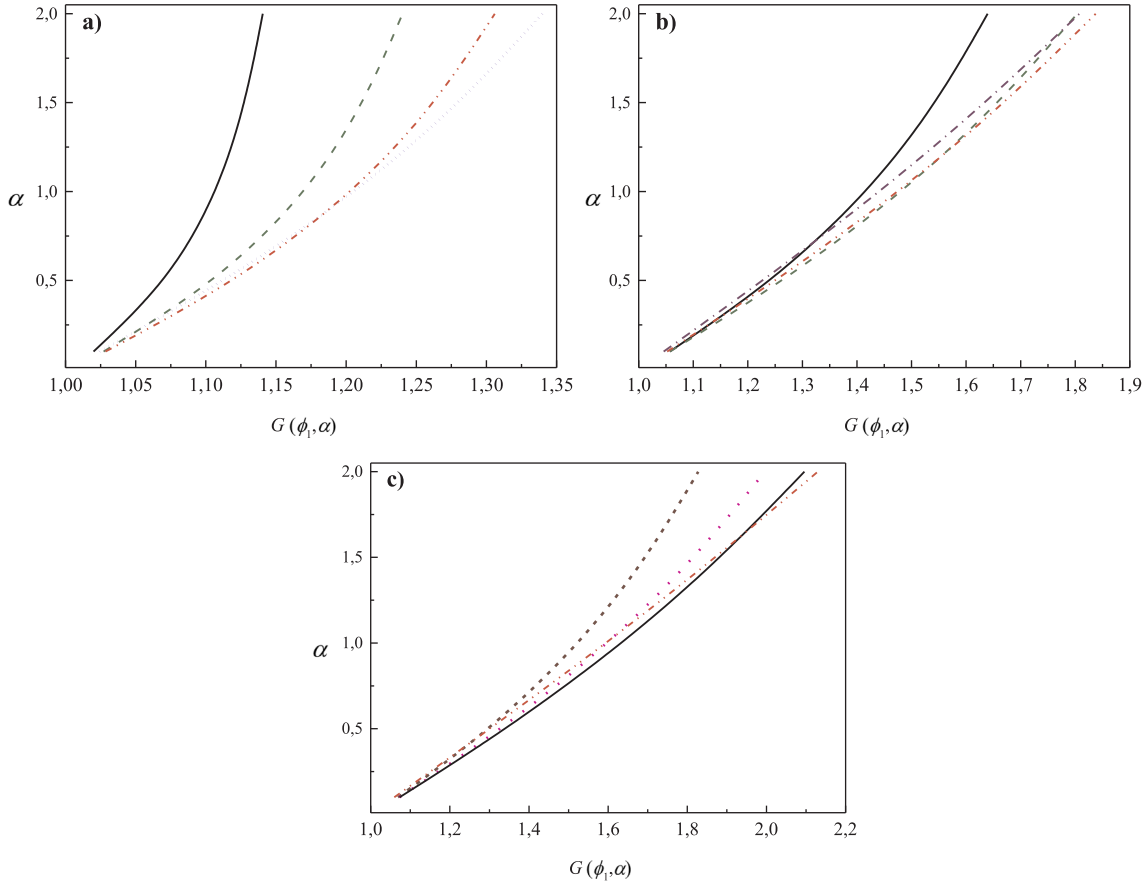

Fig. 6. Relationship between α and $G(\phi_1,\alpha)$ at various ϕ_1. Lines: $\phi_1 = 0.6$ (*short dash*), $\phi_1 = 0.8$ (*dot*), $\phi_1 = 1$ (*solid*), $\phi_1 = 1.5$ (*dash*), $\phi_1 = 2$ (*dash dot dot*), $\phi_1 = 2.5$ (*dash*), $\phi_1 = 3$ (*short dot*). a) $m = 2$, b) $m = 5$, c) $m = 10$.

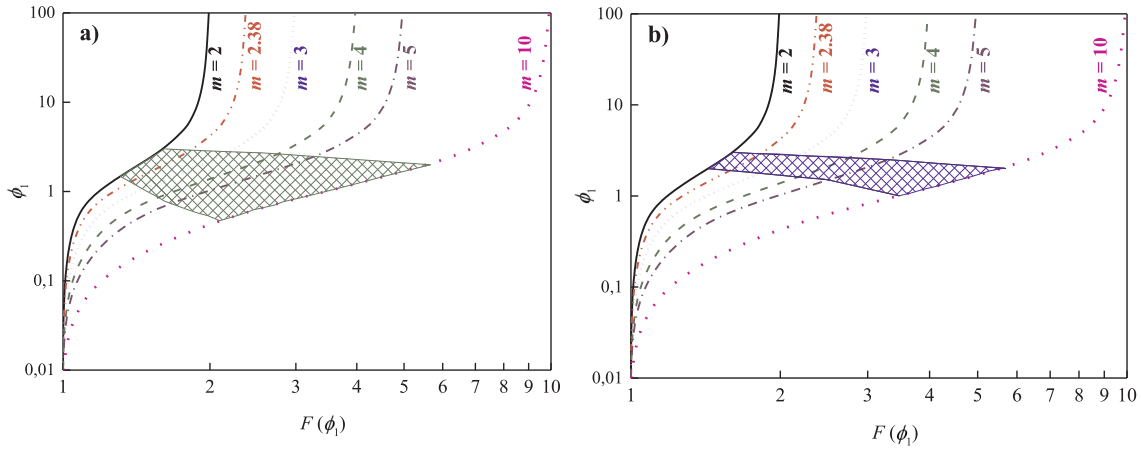

Fig. 7. Thiele modulus ϕ_1 as a function of $F(\phi_1)$ (Eq. (19)) for: a) $0.1 < \alpha < 1$, b) $0.1 < \alpha < 2$. The shaded areas indicate the method's operational windows.

- Particle size R_2:

$$t_{obs\,2} = 70.000\ s \tag{30}$$

$$\chi^*_{02} = C^*_{02}/C^0_f = 0.866 \tag{31}$$

$$R^2 = 0.9999. \tag{32}$$

In this way,

$$G(\phi_1,\alpha) = \frac{C^*_{02}}{C^*_{01}} = 1.120, \tag{33}$$

and

Table 1
Catalyst properties.

BET specific surface area (m^2/g)	343
Total pore volume (cm^3/g)	0.699
BJH Average mesopore diameter (Å)	93
Particle density (kg/m^3)	758
Porosity (ε_p, m^3/m^3)	0.530

$$F(\phi_1) = \frac{t_{obs\,2}}{t_{obs\,1}}\frac{C^*_{02}}{C^*_{01}} = 1.466. \tag{34}$$

The experimental results and the values shown in Tables 1 and 2 allow

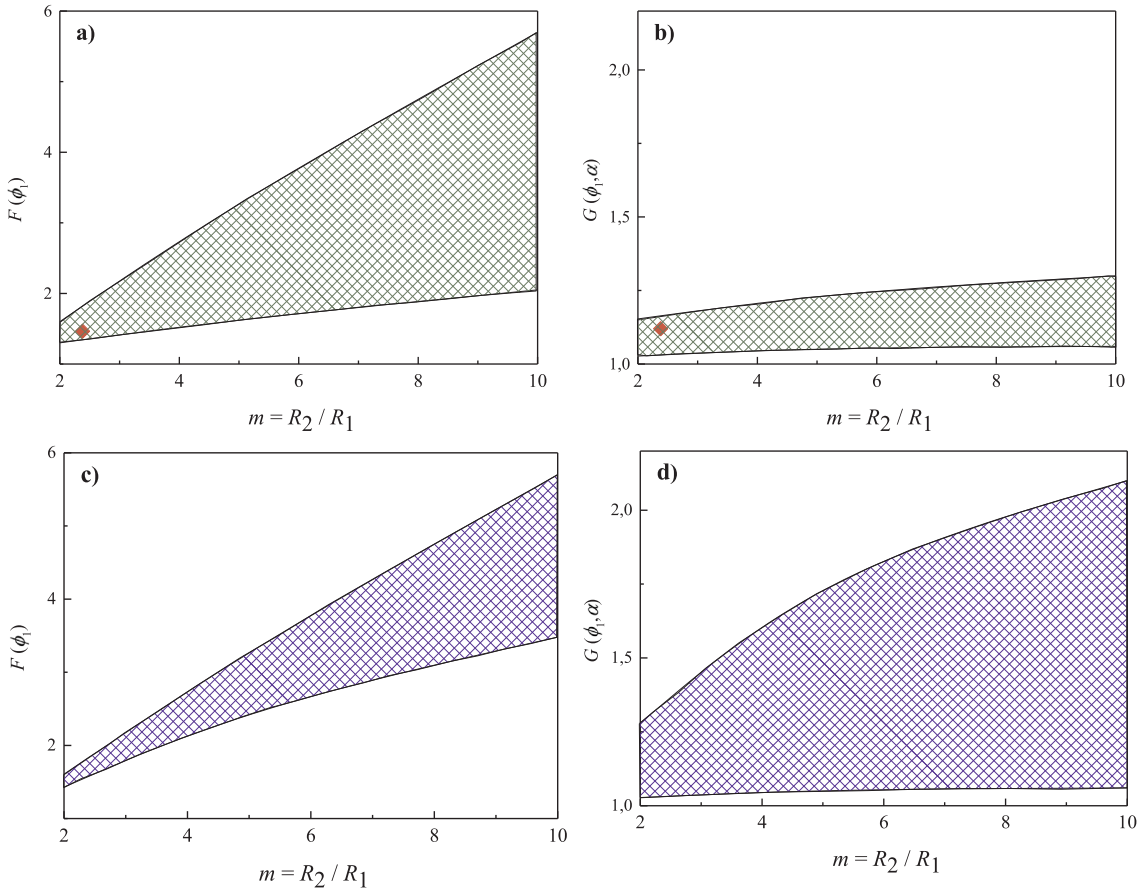

Fig. 8. $F(\phi_1)$ and $G(\phi_1,\alpha)$ as a function of m. The shaded areas indicate the recommended zones when $0.1 < \alpha < 1$ (a and b) and when $0.1 < \alpha < 2$ (c and d). The point in Fig. 8a and b refers to the experimental example (see Section 3.3.2.).

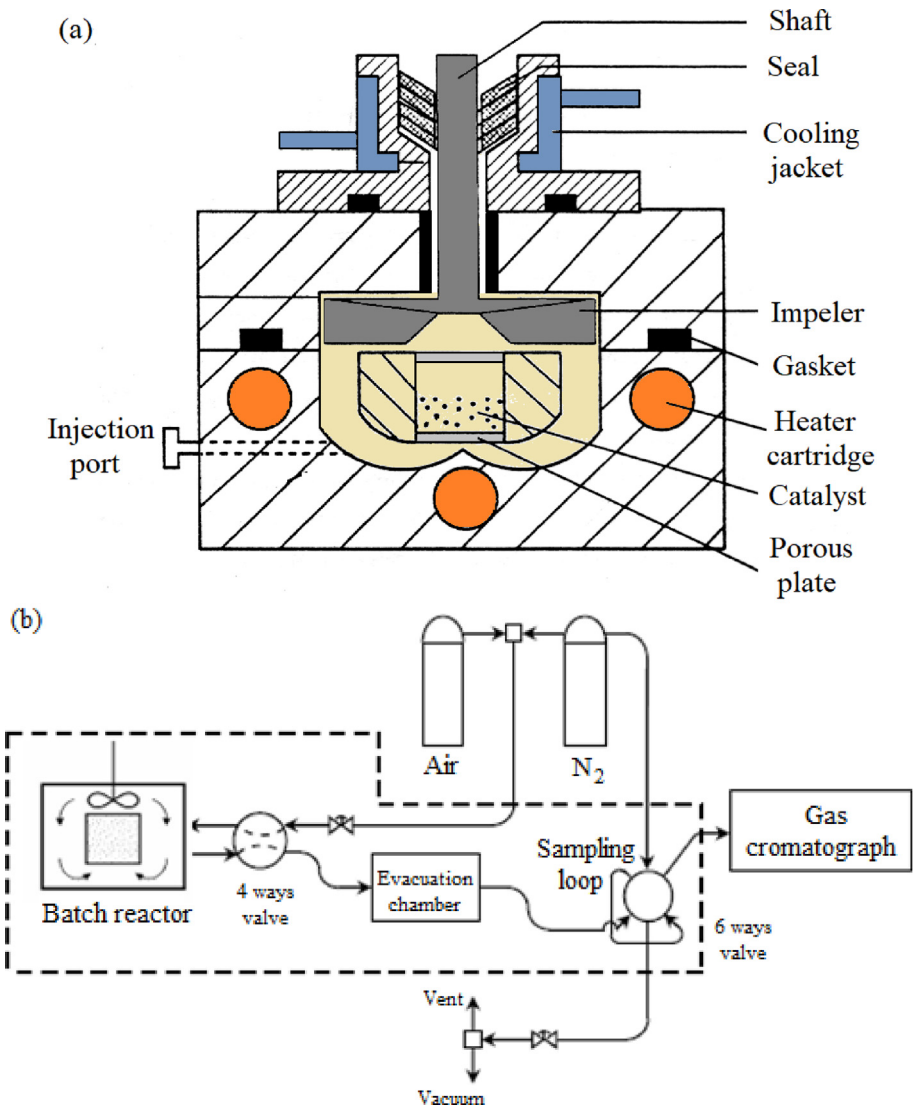

Fig. 9. Schematic representation of the CREC Riser Simulator reactor. a) Reactor; b) Experimental set-up.

Table 2
Experimental conditions in the conversion of TIPB.

Smallest particle size, average	R_1 (m)	3.2×10^{-5}
Size ratio	m (dimensionless)	2.38
Volume of reactor	V_R (m^3)	4.69×10^{-5}
Reaction time	t (s)	5–30
Mass of catalyst	m_c (kg)	5.0×10^{-4}
Volume of catalyst particles in the reactor	V_p (m^3)	6.60×10^{-7}
Mass of reactant injected	m_{TIPB} (kg)	4.1×10^{-5}

calculating the various parameters that characterize the system. Given that the relationship between the two particle sizes is known ($m = R_2/R_1 = 2.38$), the only unknown in Eq. (25) is ϕ_1. The value of the Thiele modulus for the smallest catalyst particles leading to $F(\phi_1) = 1.466$ is $\phi_1 = 1.553$, and for the largest ones is $\phi_2 = m\phi_1 = 3.701$. It is possible to calculate the corresponding effectiveness factors under the assumption of steady state by means of the classical approach [6], which are $\eta^{ss}_{(\phi 1)} = 0.869$ and $\eta^{ss}_{(\phi 2)} = 0.593$, respectively. Consequently, given that $G(\phi_1,\alpha) = C^*_{02}/C^*_{01} = 1.120$, the value of α satisfying Eq. (23) is 0.404.

The constant value of the transient effectiveness factor once the pseudo-steady state condition was reached, η^{ts}_{pE}, can be calculated very precisely by means of the approximation given by Eq. (8) [11]. Then,

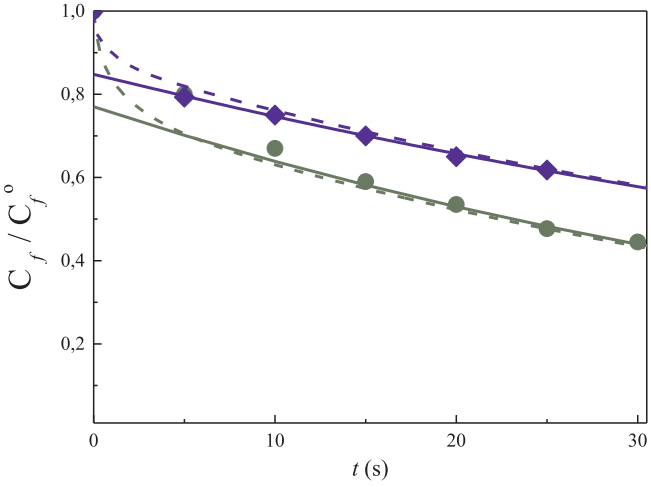

Fig. 10. Experimental evolutions of the dimensionless fluid phase concentration in the cracking of TIPB at 550 °C over particles with sizes $R_1 = 3.2\ 10^{-5}$ m (●) and $R_2 = 7.6\ 10^{-5}$ m (◆). Lines: solid, exponential fitting (Eq. (10)); dash, exact solution of the model with $D_p = 8.45 \times 10^{-10}$ m^2/s, $K = 59.05$ and $k_s = 0.0716$ 1/s.

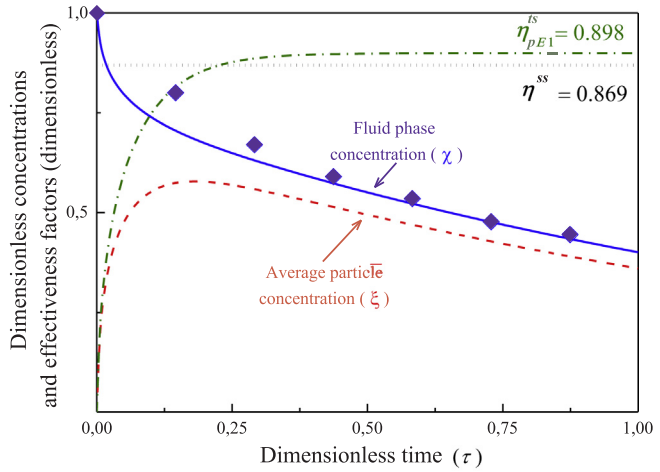

Fig. 11. Evolution of the system concentrations and effectiveness factors as a function of time. Simulations for particles with size R_1 (ϕ_1 = 1.553; α = 0.404). Lines: *solid*, χ; *dash*, $\bar{\xi}$; *dash dot*, η^{ts}; *dot*, η^{ss}. Symbols: ◆, χ (experimental observations).

$\eta^{ts}_{pE1} \cong \eta^{ts}_{Approx\,1} = \eta^{ss}_{(\phi 1)} I_{a\,(\phi 1,\alpha)} = 0.898$.

The Weisz-Prater parameter for the smallest catalyst particles can now be calculated directly from Eq. (15)

$$\theta_1 = \frac{\eta^{ts}_{pE1}\phi_1^2}{1+\alpha\,\eta^{ts}_{pE1}} = 1.589 \tag{35}$$

which allows calculating the diffusion coefficient (see Weisz-Prater parameter's definition, Eq. (14)), which is $D_p = 8.45 \times 10^{-10}\,m^2/s$. Then, the adsorption parameter K_e can be assessed from the definition of the system's adsorption capacity, $K_e = \alpha(V_f/V_p) = 28.30$ (see Eq. (A.10)). Given that the porosity in the particles is known (Table 1), the equilibrium adsorption constant is provided by Eq. (6) $K = (K_e - \varepsilon_p)/(1-\varepsilon_p) = 59.05$.

Finally, the definition of the Thiele modulus (Eq. (A.9)) shows that $k_e = (\phi_1/R_1)^2(D_p/K_e) = 0.0703$ 1/s, from where the intrinsic kinetic constant is calculated from Eq. (5), resulting $k_s = 0.0716$ 1/s.

The resulting value of D_p is in close agreement with the theoretical estimation of Knudsen diffusion coefficient [3], with a typical porosity/tortuosity factor ratio of about 0.1. It is, as expected, much larger than the diffusivities determined for zeolite catalysts [21,22].

Fig. 11 shows the evolutions of the reactant concentration, both in the fluid phase (χ), which is compared against the experimental observations, and volume averaged in the catalyst particles ($\bar{\xi}$), as simulated for the R_1 size particles. The transient (η^{ts}) and steady state (η^{ss}) effectiveness factors were also included.

As it can be seen in Fig. 8, the experimental conditions in this example (see point in the figure) are appropriate to determine the parameters characterizing the system. It can be observed in Fig. 5, with $m = R_2/R_1 = 2.38$, that $F(\phi_1) = 1.466$, as obtained from the experimental information, is very close to the value producing the minimum error propagation in the calculation of ϕ_1. Fig. 8b shows that $G(\phi_1,\alpha) = 1.120$, also from the experimental information, is located in the proper zone, in turn yielding $\alpha = 0.404$, that is, a low-medium system's adsorption capacity.

4. Conclusions

Kinetic, equilibrium and transport parameters can be determined under reaction conditions in porous catalytic particles based on a pseudo-homogeneous model, which includes the concept of transient effectiveness factor. The method is based on the use of experimental magnitudes observed in a few experiments with different catalyst particle sizes in a well stirred batch reactor where a first order chemical reaction occurs under diffusion control conditions.

If the accumulation of reactant in the catalyst particles is considered, the transient effectiveness factor allows analyzing the time response of systems with different adsorption capacities. Once a period elapsed after the pulse reactant injection, the transient effectiveness factor reaches a pseudo-equilibrium state under which an analytical expression can be used to describe the evolutions of the reactant concentration, both in the fluid phase and averaged in the solid, as a function of time. The parameters characterizing the dynamic response of the reactor according to the pseudo-homogeneous model, that is, the exponential decaying constant and the concentration extrapolated at time zero, allow using data from a few experiments to determine the system's diffusion, adsorption and chemical reaction parameters.

The case example of the conversion of 1,3,5-tri-isopropylbenzene over a silica-alumina catalyst with two different particle sizes showed that when the D_p, K and k_s parameters obtained with the proposed method are used in the exact and pseudo-homogeneous model mass balances, the corresponding evolutions of the concentrations closely agree with the experimental observations.

The approach is independent of the system's adsorption capacity, thus being applicable to cases where the assumption of steady state concentration profiles in the catalyst particles is no longer admissible. The analysis basis and the consequent methodology are more general than those resulting from the conventional assumption, which considers that the concentration profiles in the particles fulfill the steady state condition. The particular case of extremely low adsorption capacity constitutes a limiting case in the model, which enables to determine the coefficient D_p and the product Kk_s (not the isolated parameters) by means of classical approaches considering steady state in the catalyst particles. Moreover, provided the diffusive coefficient is previously known, the method also enables to determine the kinetic constant and the adsorption equilibrium parameter after experiments performed with a single particle size.

Acknowledgement

The financial support of Universidad Nacional de Mar del Plata (UNMdP, Project ING 448/16), Universidad Nacional del Litoral (UNL, Project CAID 2011 #50120110100546), National Scientific and Technical Research Council CONICET (PIP 593/13) and the National Agency for Scientific and Technological Promotion, (ANPCyT, PICT 2010/2123) is gratefully acknowledged.

Appendix A

The mass balance for the reactant in the catalyst particles can be written as

$$\varepsilon_p \frac{\partial C}{\partial t} = \varepsilon_p D \nabla^2 C - (1-\varepsilon_p)\frac{\partial Q}{\partial t} - (1-\varepsilon_p) k_s Q \tag{A.1}$$

where $Q = K\,C$ is the concentration of reactant adsorbed in the solid. If Eq. (A.1) is expressed in terms of the concentration of reactant diffusing through the particle pores, the balance can be written as

$$\frac{\partial C}{\partial t} = D_e \nabla^2 C - k_e C \tag{A.2}$$

subjected to the following boundary and initial conditions:

$$C_{(r,0)} = 0 \tag{A.3}$$

$$\left.\frac{\partial C}{\partial r}\right|_{r=0} = 0 \tag{A.4}$$

$$C_{(R,t)} = C_{f(t)} \tag{A.5}$$

with $D_e = D_p/K_e = \varepsilon_p D/K_e$, $k_e = (1-\varepsilon_p)Kk_s/K_e$ and $K_e = \varepsilon_p + (1-\varepsilon_p)K$. K is the Henry's adsorption constant (linear equilibrium) of the reactant, k_s is the first order reaction rate constant and $D_p = \varepsilon_p D$ is the diffusivity in the particle, which can be evaluated from the estimation of the Knudsen and molecular diffusion coefficients and the tortuosity factor [23].

The overall mass balance in the reactor is

$$V_f \frac{dC_f}{dt} = -V_p \frac{3}{R}\varepsilon_p D \left.\frac{\partial C}{\partial r}\right|_{r=R} \tag{A.6}$$

subjected to the following initial condition:

$$C_{f\,(t=0)} = C_f^o. \tag{A.7}$$

If dimensionless variables are used according to

$$\tau = \frac{tD_e}{R^2}, \quad \rho = \frac{r}{R}, \quad \xi = \frac{C}{C_f^o}, \quad \chi = \frac{C_f}{C_f^o}, \tag{A.8}$$

where C_f^o is the initial concentration ($=N^o/V_f$), the following parameters can be defined

$$\phi = R\sqrt{\frac{k_e}{D_e}}, \tag{A.9}$$

$$\alpha = \frac{V_p K_e}{V_f}. \tag{A.10}$$

The parameter ϕ is the well-known Thiele modulus and the parameter α is the system's adsorption capacity, which relates the magnitudes of the capacities of the solid and fluid phases to retain reactant [10].

By using Eqs. (4)(6), (A.8) and (A.9) into Eqs. (A.2)(A.7) their corresponding dimensionless forms are given by Eqs. (1)(3).

The solution of the system of Eqs. (1)(3) provides the profiles of concentration of reactant in the spherical particles as a function of the dimensionless time $\xi = f(\rho,\tau)$ for given parameters ϕ and α. Additionally, the evolution of the concentration of reactant in the fluid phase $\chi = f(1,\tau)$ is obtained. Once the problem has been solved, it is easy to find the volume average concentration of reactant in the pores of the catalyst particles

$$\bar{\xi} = 3\int_0^1 \xi \rho^2 d\rho. \tag{A.11}$$

Appendix B

Eq. (A.2), averaged in the particles' volume, is

$$\frac{d\overline{C}}{dt} = \frac{1}{V_p}\int_{V_p} D_e \nabla.\,(\nabla C)dV - k_e\overline{C}. \tag{B.1}$$

If the Gauss' theorem is applied on the first term in the right hand side of Eq. (B.1),

$$\frac{1}{V_p}\int_{V_p} D_e \nabla.\,(\nabla C)dV = \frac{3}{R}D_e \left.\frac{\partial C}{\partial r}\right|_{r=R} \tag{B.2}$$

and then

$$\frac{3}{R}D_e \left.\frac{\partial C}{\partial r}\right|_{r=R} = \frac{d\overline{C}}{dt} + k_e\overline{C} \tag{B.3}$$

or

$$\frac{3}{R}\varepsilon_p D \left.\frac{\partial C}{\partial r}\right|_{r=R} = K_e\left[\frac{d\overline{C}}{dt} + k_e\overline{C}\right]. \tag{B.4}$$

If Eq. (B.4) is used in the mass balance in the reactor (Eq. (A.6)) it yields

$$V_f \frac{dC_f}{dt} = -V_p K_e\left[\frac{d\overline{C}}{dt} + k_e\overline{C}\right] \tag{B.5}$$

which can be written in its dimensionless form by means of Eq. (A.8)(A.10)

$$\frac{d\chi}{d\tau} = -\alpha\left[\frac{d\bar{\xi}}{d\tau} + \phi^2\bar{\xi}\right]. \tag{B.6}$$

It was shown that the volume average concentration in the particle ($\bar{\xi}$, Eq. (A.11)) can be expressed by means of a series expansion in terms of the

fluid phase concentration of reactant (χ) and its derivatives [16]

$$\bar{\xi} = s_1\chi - s_2\frac{d\chi}{d\tau} + s_3\frac{d^2\chi}{d\tau^2} - \ldots + \sum_{n=1}^{\infty}\left(\frac{e^{-\lambda_n\tau}}{\lambda_n}\right)\left(-\chi_{(\tau=0)} + \frac{1}{\lambda_n}\frac{d\chi}{d\tau}\bigg|_{(\tau=0)} - \frac{1}{\lambda_n^2}\frac{d^2\chi}{d\tau^2}\bigg|_{(\tau=0)} + \ldots\right) \tag{B.7}$$

with

$$s_i = \sum_{n=1}^{\infty}\frac{6}{\lambda_n^i}, \tag{B.8}$$

where the eigenvalues λ_n are

$$\lambda_n = \phi^2 + n^2\pi^2. \tag{B.9}$$

The exponential terms in Eq. (B.7) can be considered negligible if the time elapsed is longer than $\tau > 1/(\pi^2 + \phi^2)$. Then, Eq. (B.7) becomes

$$\bar{\xi} = s_1\chi - s_2\frac{d\chi}{d\tau} + s_3\frac{d^2\chi}{d\tau^2} - \ldots \tag{B.10}$$

If Eq. (B.10) is truncated in the second term

$$\frac{d\chi}{d\tau} \cong \frac{1}{s_2}(s_1\chi - \bar{\xi}). \tag{B.11}$$

The derivative of Eq. (B.10) is

$$\frac{d\bar{\xi}}{d\tau} = s_1\frac{d\chi}{d\tau} - s_2\frac{d^2\chi}{d\tau^2} + s_3\frac{d^3\chi}{d\tau^3} - \ldots \tag{B.12}$$

and, neglecting the terms corresponding to the second and higher order derivatives,

$$\frac{d\bar{\xi}}{d\tau} \cong s_1\frac{d\chi}{d\tau}. \tag{B.13}$$

If Eqs. (B.11) and (B.13) are used in the overall mass balance for the reactant in the reactor (Eq. (B.6)), the dimensionless average reactant concentration in the particle can be obtained,

$$\bar{\xi} = s_1\left[\frac{(1 + \alpha s_1)}{1 + \alpha s_1 - \alpha s_2\phi^2}\right]\chi. \tag{B.14}$$

From Eqs. (B.8) and (B.9) it can be seen that the coefficient s_1 in this equation is

$$s_1 = \sum_{n=1}^{\infty} 6/(\phi^2 + n^2\pi^2) = \frac{3}{\phi^2}(\phi\coth\phi - 1) = \eta^{ss} \tag{B.15}$$

i.e., the steady state effectiveness factor (η^{ss}). The term between brackets in Eq. (B.14) is

$$I_a = \frac{(1 + \alpha s_1)}{1 + \alpha s_1 - \alpha s_2\phi^2}. \tag{9}$$

According to Eq. (7) the transient effectiveness factor is given by the relationship between $\bar{\xi}$ and χ which, after an initial period (see Fig. 1), becomes constant. Then, as it can be derived from Eqs. (7) and (B.14),

$$\eta_{pE}^{ts} = \frac{\bar{\xi}}{\chi}\bigg|_{\tau > 1/(\pi^2+\phi^2)} = s_1\left[\frac{(1 + \alpha s_1)}{1 + \alpha s_1 - \alpha s_2\phi^2}\right] = \eta^{ss}I_a. \tag{B.16}$$

Eq. (B.16) shows that the correction factor I_a represents the relationship between the constant value of the transient effectiveness factor (η_{pE}^{ts}) and the steady state effectiveness factor (η^{ss}) in a well stirred batch reactor. I_a considers the accumulation term in the particles and is always higher than one due to inertia of the particles to respond to the changes in the fluid phase concentration [10].

References

[1] H.S. Fogler, Elements of Chemical Reaction Engineering, third ed. Prentice-Hall Englewood Cliffs, New Jersey, 1999.
[2] T. Furusawa, M. Suzuki, J.M. Smith, Rate parameters in heterogeneous catalysis by pulse techniques, Catal. Rev. Sci. Eng. 13 (1) (1976) 43–76.
[3] G. Froment, K. Bischoff, J. De Wilde, Chemical Reactor Analysis and Design, third ed., John Wiley and Sons Inc., New York, 2011.
[4] T. Titze, Ch. Chmelik, J. Kullmann, L. Prager, E. Miersemann, R. Gläser, D. Enke, J. Weitkamp, J. Kärger, Microimaging of transient concentration profiles of reactant and product molecules during catalytic conversion in nanoporous materials, Angew. Chem. Int. Ed. 54 (2015) 5060–5064.
[5] V. Weekman, Laboratory reactors and their limitations, AIChE J. 20 (1974) 833–840.
[6] E. Thiele, Relation between catalytic activity and size of particle, Ind. Eng. Chem. 31 (1939) 916–920.
[7] R. Aris, The Mathematical Theory of Diffusion and Reaction in Permeable Catalyst, first ed., Oxford University Press, New York, 1975.
[8] P.B. Weisz, C. Prater, Interpretation of Measurements in Experimental Catalysis, in: W. Frankenburg, V. Komarewsky, E. Rideal (Eds.), Advances in Catalysis, Academic Press, New York, 1954, pp. 143–196.
[9] C.M. Bidabehere, U. Sedran, Use of stirred tank reactors for the assessment of adsorption constants in porous solid catalysts with simultaneous diffusion and reaction. Theoretical analysis, Chem. Eng. Sci. 61 (2006) 2048–2055.
[10] C.M. Bidabehere, J.R. García, U. Sedran, Transient effectiveness factors in the dynamic analysis of heterogeneous reactors with porous catalyst particles, Chem. Eng. Sci. 137 (2015) 293–300.
[11] C.M. Bidabehere, J.R. García, U. Sedran, Transient effectiveness factors in porous catalyst particles. Application to kinetic studies with batch reactors, Chem. Eng. Res. Des. 118 (2017) 41–50.
[12] E. Miró, D. Ardiles, E. Lombardo, J. Petunchi, Continuous –stirred tank reactor (CSTR) transient studies in heterogeneous catalysis. CO oxidation over CuY zeolite, J. Catal. 97 (1986) 43–51.
[13] D. Kim, D. Park, J. Lee, Preferential CO oxidation over CuO-CeO_2 in excess hydrogen: effectiveness factors of catalyst particles and temperature window for CO

removal, Int. J. Hydrogen Energy 38 (2013) 4429–4436.
[14] A. Dursun, O. Tepe, Internal mass transfer effect on biodegradation of phenol by Ca–alginate immobilized *Ralstonia eutropha*, J. Hazard. Mater. 126 (2005) 105–111.
[15] J.L. Gomez Carrasco, E. Gomez Gomez, M. Gomez Gomez, M. Murcia, S. Ortega Requena, A diffusion-reaction kinetic model for the removal of aqueous 4-chlorophenol with immobilized peroxidase, Chem. Eng. J. 166 (2011) 693–703.
[16] D. Kim, Linear driving force formulas for diffusion and reaction in porous catalysts, AIChE J. 35 (1989) 343–346.
[17] D. Kim, Linear driving force formulas for unsteady-state diffusion and reaction in slab, cylinder and sphere catalyst, AIChE J. 33 (2009) 834–839.
[18] W.F. Ames, Numerical Methods for Partial Differential Equations, first ed., Academic Press, New York, 1975.
[19] J.R. García, C.M. Bidabehere, U. Sedran, Diffusion controlled LHHW kinetics. Simultaneous determination of chemical kinetic and equilibrium adsorption constants by using the Weisz-Prater approach, Chem. Eng. Sci. 172 (2017) 444–452.
[20] H. de Lasa, Novel Riser Simulator Reactor. US Patent 5.102.628, 1992.
[21] N. Tukur, S. Al-Khattaf, Catalytic cracking of n-dodecane and alkyl benzenes over FCC zeolite catalysts: time on stream and reactant converted models, Chem. Eng. Proc. 44 (2005) 1257–1268.
[22] M. Al-Sabawi, H. de Lasa, Modeling thermal and catalytic conversion of decalin under industrial FCC operating conditions, Chem. Eng. Sci. 65 (2010) 626–644.
[23] C. Satterfield, Mass Transfer in Heterogeneous Catalysis, R. E. Krieger Pub. Co., Malabar, Florida, 1981.